NANO LETTERS

Letter

pubs.acs.org/NanoLett

Tetrapod Nanocrystals as Fluorescent Stress Probes of Electrospun Nanocomposites

Shilpa N. Raja,[†,‡,#] Andrew C. K. Olson,[†,§,#] Kari Thorkelsson,[†,‡] Andrew J. Luong,[‡,⊥] Lillian Hsueh,[‡,⊥] Guoqing Chang,[∥] Bernd Gludovatz,[†] Liwei Lin,[∥] Ting Xu,[†,‡,§] Robert O. Ritchie,[†,‡,∥] and A. Paul Alivisatos[†,‡,§,*]

[†]Materials Science Division, Lawrence Berkeley National Laboratory, Berkeley, California 94720, United States

[‡]Department of Materials Science and Engineering, University of California, Berkeley, California 94720, United States

[§]Department of Chemistry, University of California, Berkeley, California 94720, United States

[⊥]Department of Chemical Engineering, University of California, Berkeley, California 94720, United States

[∥]Department of Mechanical Engineering, University of California, Berkeley, California 94720, United States

Supporting Information

ABSTRACT: A nanoscale, visible-light, self-sensing stress probe would be highly desirable in a variety of biological, imaging, and materials engineering applications, especially a device that does not alter the mechanical properties of the material it seeks to probe. Here we present the CdSe–CdS tetrapod quantum dot, incorporated into polymer matrices via electrospinning, as an *in situ* luminescent stress probe for the mechanical properties of polymer fibers. The mechanooptical sensing performance is enhanced with increasing nanocrystal concentration while causing minimal change in the mechanical properties even up to 20 wt % incorporation. The tetrapod nanoprobe is elastic and recoverable and undergoes no permanent change in sensing ability even upon many cycles of loading to failure. Direct comparisons to side-by-side traditional mechanical tests further validate the tetrapod as a luminescent stress probe. The tetrapod fluorescence stress–strain curve shape matches well with uniaxial stress–strain curves measured mechanically at all filler concentrations reported.

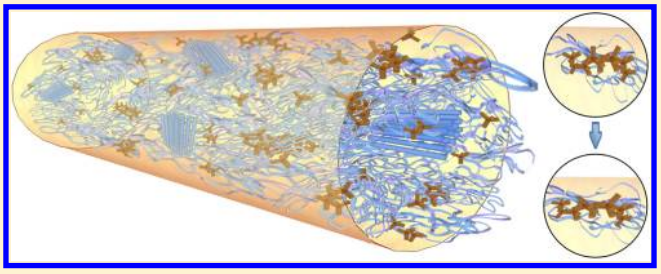

KEYWORDS: *Nanocomposite, polymer, nanocrystal, electrospinning, mechanical, sensor*

Polymer–nanoparticle composites can exhibit enhanced mechanical properties and unique functionalities,[1−10] enabling new functional materials such as antimicrobial polymers[11] and biocompatible implants.[12] However, rational design of these materials has remained elusive, due to a lack of detailed understanding of stress profiles at the microscale and nanoscale. Specifically, an understanding of the interface between the filler and polymer and how stresses are transferred across that barrier are critical in reproducibly synthesizing composites.[13−17]

Established techniques for these studies—including micro-Raman spectroscopy,[18] synchrotron radiation,[19] and electron backscattering[20] as well as contact techniques such as atomic force microscopy,[21,22] nanoindentation,[23] and others[24]—are difficult to adapt to *in vivo* stress detection and premature failure detection in service due to their stringent requirements in sample size and shape or need for controlled laboratory environments. Recent advances in smart materials have used self-reporting fillers such as near-infrared molecular probes,[25] micrometer-sized ZnO tetrapods,[26] metal nanoparticles,[27] and bioinspired concentric optical fibers with varying refractive index.[28] However, these fillers have drawbacks, including altering the molecular-level composition and structure of the polymer and potentially weakening multiple mechanical properties such as toughness. It is therefore of considerable interest to develop an optical luminescent stress sensing nanoparticle, and to establish ways of embedding these inside polymers without perturbing the mechanical properties that are being sensed. Herein, we demonstrate that it is possible to use luminescent semiconductor nanocrystal tetrapods as stress sensors, and that their dispersion inside polymer fibers at variable densities can be controlled by electrospinning, without changing the inherent mechanical behavior of the fibers.

Previous work with tetrapod Quantum Dots (tQDs)[29−31] has suggested that they have significant potential as stress sensors.[32,33] With a zinc-blende CdSe core and four epitaxially grown wurtzite CdS arms (Figure 1A), these quasi-type I heterostructures are highly emissive with quantum yields of up to 60% in the visible range.[29,30] In response to nano-Newton forces, they were predicted to have a monotonically decreasing band gap[34,35] and were shown in a diamond anvil cell experiment to have a fluorescence red shift in response to

Received: June 2, 2013
Revised: June 25, 2013
Published: July 1, 2013

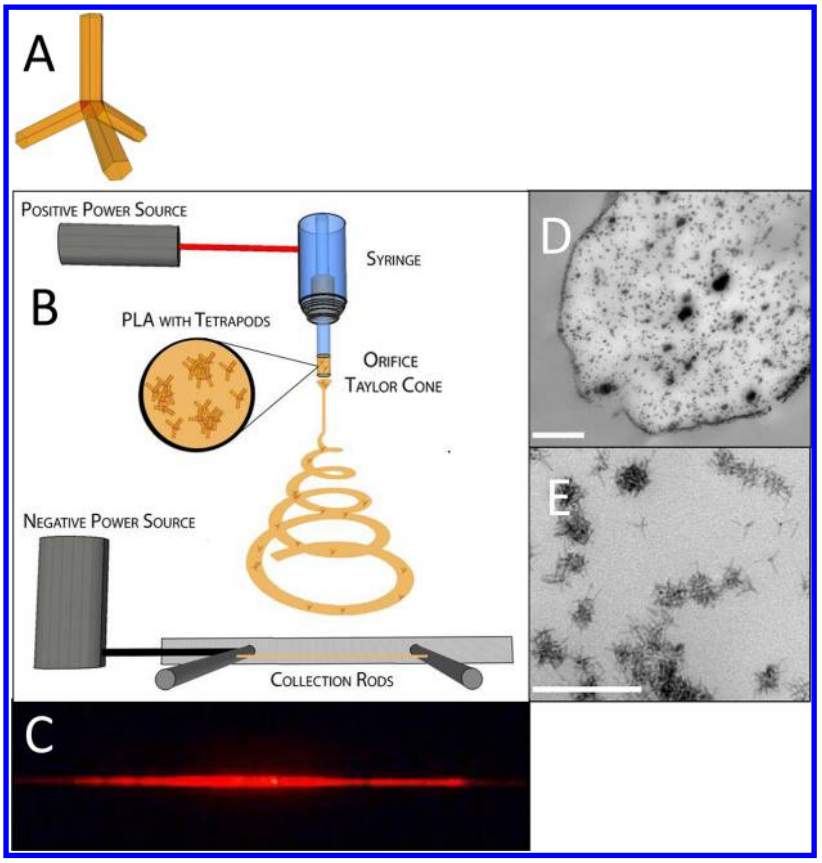

Figure 1. Preparation and visualization of tetrapod quantum dot-poly-L-lactic acid (tQD-PLLA) composite electrospun fibers. (A) Schematic of CdSe-CdS core-shell nanotetrapod with zinc blende CdSe core and wurtzite CdS shell. (B) Schematic of electrospinning process. (C) Fluorescence image of tQD-PLLA electrospun fiber. (D) TEM image of tQD-PLLA electrospun fiber cross-section (scale bar 500 nm). (E) Higher magnification view of tQD-PLLA composite shown in part C (scale bar 200 nm).

nonhydrostatic gigapascal stresses.[33] The surface chemistry of tQDs can be easily modified following established nanoparticle ligand exchange,[36] which can allow them to be easily incorporated into a wide variety of synthetic and biological polymers. Despite this, previous studies were limited by very dilute (~0.002% by weight) incorporation of these nanocrystals into polymers via diffusion.[32]

In the present work, we substantially extend the range of loading by employing electrospinning as a facile means of introducing the tQDs into the polymer. We incorporate, via electrospinning, several concentrations of tQDs (from 3.6 to 40% by weight) into poly L-lactic acid (PLLA), forming a nanocomposite material with PLLA as the polymer matrix host material, and the tQD as the nanoscale composite filler material. Optical and mechanical experiments on this nanocomposite show that the tetrapod nanocrystal sensor matches the bulk mechanical sensor with a very high degree of agreement in the basic tensile mechanical properties as well as under cyclic loading and stress relaxation. Several differences between the sensing behavior of the universal testing machine (UTM) macroscale load cell and the tQD nanoscale load cell are observed, which we attribute to an imperfect polymer-nanocrystal interface and consequent incomplete stress transfer to the tQD filler.[13] As discussed below, particle aggregation during composite formation limits stress transfer to the tetrapods, which ensures elasticity and recyclability of the probe by preventing plastic deformation of the nonperturbing (i.e., causes no change to the mechanical properties) nanoscale sensor. We further show that increasing the tetrapod concentration, while affording little to no change in the polymer mechanical and structural properties, effectively improves the tQD sensor response and sensitivity. Finally, we examine the stress relaxation and cyclic deformation/hysteresis of the polymer composites using the tQD deformation sensor.

Results and Discussion. *Nanocomposite Electrospinning.* In order to incorporate tQDS into the PLLA polymer at a large range of concentrations to investigate the impact on mechanical properties as well as the opto-mechanical self-sensing ability of the polymer nanocomposite, we used electrospinning, a versatile technique for micro- and nanofiber formation, which involves applying a large electric field (approximately 1 kV/cm or higher) to a droplet of polymer solution on the end of a syringe needle.[37−39] Upon sufficiently high electric field application, the droplet loses its spherical shape and begins to elongate, forming a shape termed the Taylor cone. Subsequently, a jet stream erupts from the unstable Taylor cone, forming fibers at the grounded electrode (Figure 1B). The large electric field may cause nanocrystals and particle aggregates to be more uniformly dispersed throughout the polymer matrix than other nanocomposite fabrication methods.[40,41] This may minimize the formation of stress concentrations within the nano/microstructure, which would act to degrade the mechanical properties of composite materials.[42,43]

Briefly, tQDs and a solution of poly L-lactic acid (PLLA) in chloroform were mixed and loaded into a 1-mL syringe with an attached #21 gauge needle. A droplet of the solution was manually ejected from the syringe immediately prior to

dx.doi.org/10.1021/nl401999t | Nano Lett. 2013, 13, 3915−3922

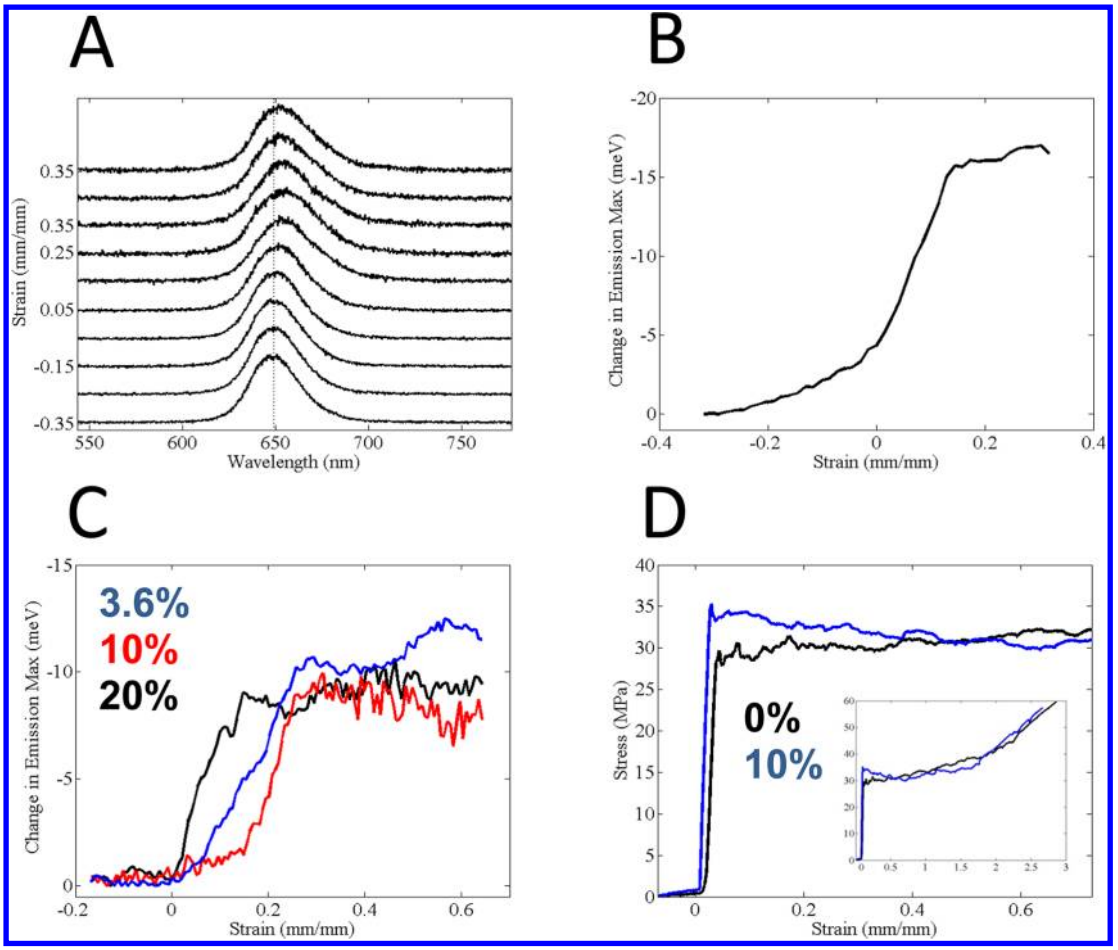

Figure 2. Comparison of tetrapod stress or strain gauge with commercial mechanical tensile testing machine (Agilent T150). (A) Selection of 10 raw spectra from a trial illustrating redshift of fluorescence emission as function of continuously imposed strain. (B) Fluorescence tensile curve obtained by fitting and plotting sequentially full set (approximately 200 spectra) of data represented in part A. Negative strain indicates slack. (C) Illustration of typical fluorescence tensile curves at three tetrapod loadings (3.6%, 10% and 20%), showing increase in slope of linear region as function of loading. The 10% curve is offset by 0.2 strain for clarity. (D) Comparative typical macroscopic uniaxial tensile curve on same batch of fibers (0% tetrapods and 10%).

applying a one kilovolt/centimeter electric field. This caused individual fibers to be formed on the dual rod electrodes[44]- (Figure 1B). The fibers dried within seconds[45] and were collected for optical and mechanical tests. Figure 1C represents a bright-field fluorescence image of a resulting electrospun fiber, showing red 650 nm fluorescence from the tetrapods dispersed throughout the fiber. No diffusion of the fluorescence intensity along the length of the fiber during tests was observed, leading us to conclude that the tetrapods are effectively incorporated into the polymer composite structure. The tetrapods are not covalently bound to the matrix, nor have they undergone ligand exchange. They are simply incorporated into the polymer via electrospinning with their native hydrophobic ligands. Tetrapods were incorporated at concentrations of 0, 3.6, 10, 20, and 40% by weight of the PLLA polymer. Parts D and E of Figure 1 show the polymer−tetrapod fiber TEM images where the tetrapods are mostly forming aggregates in the fiber. Particles and aggregates show no preference for the PLLA−solvent interface or interior of the fiber.

Fluorescence Monitoring of Tensile Deformation. After collection, fibers were mounted onto the piezodrive *in situ* stretcher for fluorescence tests or onto cardboard tabs for mechanical tests. Figure 2A shows the raw spectra from a typical fluorescence test, indicating both a redshift as well as an increase in the full-width half-maximum (fwhm) of the fluorescence spectrum as a function of stretching. As previously discussed, red-shifts in fluorescence during extension cannot be explained by polymer heating or changes in refractive index.[32] The increase in fwhm (10−20% increase) may be due to a combination of innate spectral line broadening during tetrapod nanocrystal deformation and the natural heterogeneity of strain states within the PLLA polymer fiber. The deformation of the tQD leads to bending of the CdS arms which stretches some bonds more than others; for example, the bonds at the interface between the arm and the CdSe core are more stretched than bonds within the CdSe core. Additionally, the tetrapods at an aggregate edge may be experiencing a different stress than the ones in the middle of a clump or smaller groups of particles in different mechanical contact with the polymer. In the absence of single nanocrystal photoluminescence studies in the fibers, it is not yet known to what degree deformation of an individual nanocrystal broadens its emission, so the relative contribution of these mechanisms to the fwhm broadening is unclear.

However, the redshift in peak emission clearly tracks fiber deformation. Figure 2B shows the result of fitting the spectra in Figure 2A to single Gaussians and then plotting these as a function of strain. It indicates an initial slack region followed by a linear elastic region, which then yields and flattens out into a

dx.doi.org/10.1021/nl401999t | *Nano Lett.* 2013, 13, 3915−3922

plastic regime. This result matches textbook polymer tensile test graphs,[46] as well as our own mechanical tests conducted on the same batch of fibers.

Concentration Dependence on Sensing Ability. Figure 2C indicates that as the concentration of tetrapods in the polymer increases, tQD sensitivity to strain in the fiber increases as evidenced by the average slopes of the linear region. Between concentrations of 3.6 to 20% by weight of the tQDs in the polymer, the average fluorescence slope (ΔmeV/strain) increases 60% from 39 to 62, though the general shape of the tensile curves is constant (see Supporting Information, Table S3, for linear regression). The observed clear distinction between elastic and plastic regimes and consistent curve shape across all particle concentrations in fluorescence tests has not been reported previously.[26,32] Although optical and mechanical tests were conducted on different fibers, all nanocomposite fibers used in comparative tests came from the same batch of electrospun fibers prepared using the same tQDs and polymer precursor solutions.

Fiber-polymer composite studies[47−49] help explain the concentration-dependence illustrated in Figure 2C. It is commonly observed in fiber-polymer composites that, provided the fiber/matrix interface is sufficiently strong, the larger the fiber aspect ratio the better the stress transfer and the better the overall composite properties up to a critical length.[47−49] Our observation of a fluorescence slope increase with increased tQD concentration is similar. As the filler concentration increases, the average aggregate size increases and the spacing between aggregates decreases, analogous to a larger aspect ratio in ceramic fiber-polymer composites. This augmented interaction between aggregates leads to a greater stress transfer to the tetrapod phase of the composite. A similar result was recently reported with micrometer-sized ZnO tetrapods, though in that case a clear distinction between elastic and plastic regimes and good resemblance between tensile and fluorescence curve shapes was only seen at high (50% by weight) ZnO tetrapod concentrations.[26] In contrast, we see clear a distinction between elasticity and plasticity and an optical response approaching that in the mechanical tests at tQD concentrations as low as 3.6% by weight of the polymer. Additionally, in the work with ZnO tetrapods, oscillations were seen in the fluorescence tests at low tetrapod concentrations; this was attributed to noninterlocked tetrapod domains in the polymer matrix.[26] In our case, we find oscillation-free behavior at even the lowest tQD concentrations in the polymer, meaning that interlocking is not necessary to achieve curves with relatively low noise and reasonable accuracy.

A complementary explanation for the particle concentration dependence shown in Figure 2C is that aggregates near the fiber surface experience increased local strain due to the Poisson effect. PLLA has a Poisson's ratio of ∼0.4,[50] indicating that it contracts roughly one unit radially for every two units extended axially. Studies indicate that the Poisson's ratio is larger near the surface of a fiber;[51] thus, this contracting force will be greatest at the surface. As the aggregate concentration increases, the number of aggregates proximal to the outer surface of the fiber does as well (Figures S1−S2, Supporting Information). Consequently, more aggregates are present in the region of maximum contracting force near the surface, leading to larger stress transfer and thus better response of the tQD probe. This explanation is consistent with the fact that the average maximum fluorescence peak shift also was seen to increase with concentration from −9.5 meV to −11.3 meV for 3.6% to 20% tQD concentrations by weight in the polymer, respectively, indicating that the sensor becomes more sensitive with increasing concentration.

Unchanged Mechanical and Structural Properties: A Non-Perturbing Probe. Somewhat surprisingly, the ceramic tetrapods do not significantly affect the mechanical properties of the nanocomposite, even at high tQD concentrations. Figure 2D shows comparative uniaxial tensile stress−strain curves of electrospun PLLA with and without tQDs and qualitative agreement with optical curves (Figure 2C). The inset of Figure 2D shows the full mechanical curves to failure for the same fibers, indicating close agreement between different concentrations, even for 20% by weight tetrapod-fiber nanocomposites. We discuss a possible explanation for the unique nonperturbing behavior of the tQD probe below. The oscillation inherent to the flat region of the polymer curves at high strain is due to plastic deformation; local molecular variations in polymer stress as strands unravel and molecular-scale rearrangements during neck extension. These variations are captured in both the optical and mechanical data.

From the mechanical tests performed on the tensile testing machine on a total of over 70 fibers, there is no significant trend in modulus (measured by taking the slope of the initial linear elastic region of the engineering stress−strain curve), toughness (measured by taking the area under the curve of the entire engineering stress−strain curve), or stress and strain at failure with concentration increased from 0% to 20% by weight of tetrapods in the PLLA polymer. Even at 40%, there is no significant change in elastic modulus although there is a decrease in toughness and other mechanical properties (Supporting Information, Table S1). This is unusual as many composite systems of semiconductor quantum dots,[52−55] micrometer-scale tetrapods,[26] and other polymer−ceramic systems[56] show modulus increases with such weight percent additions, sometimes accompanied by decreases in failure strains and toughness. Although opposite effects have also been observed,[13] it is perhaps surprising that all the tensile mechanical properties remain relatively unchanged with such high concentration of tetrapods. However, we believe that this is due to the combination of the weak tQD−polymer interface and PLLA structural variations caused by electrospinning. The poor stress transfer due to the weak interface explains why the measured Young's moduli do not follow a straightforward "rule of mixtures" analysis.[57] Regarding structural variations, PLLA is a semicrystalline polymer with multiple phases determining its mechanical properties. These phases can clearly be observed as darker and lighter (crystalline and amorphous) regions in our transmission electron microscopy (TEM) images. Small changes in the processing of the electrospinning precursor solutions, such as those introduced by large particle loading, may impact the crystallinity of the resultant fibers. Collection conditions as well as inherent electric field variations across the dual-rod electrodes may also result in structural variations. Accordingly, dynamic scanning calorimetry (DSC) analysis showed significant variation in crystallinity and grain size across samples, but no net effects on the crystallinity and polymer structural and thermal properties as a function of tQD concentration in the nanocomposite (Supporting Information, Table S1). The result is a material that shows little change in a wide range of mechanical properties even at large particle volume fractions.

Incomplete Stress Transfer to Nanofiller Sensor. It is apparent from parts B and D of Figure 2 that the linear elastic

region as measured by the tQD sensor is much broader and covers more strain (6−30% extension) than the linear elastic region as measured by the UTM (which covers between 1 and 3%). We speculate that this is due to poor stress transfer to the tQD filler. In the case of strong stress transfer, we would expect fluorescence shifts to occur over the same range of strain as seen in the mechanical data as well as significant mechanical property changes in the nanocomposite.[58,59] The poor stress transfer is due to a weak interface between the nanocrystal and the polymer. The PLLA polymer is a hydrophilic aliphatic polyester with hydrogen bonding between the chains. The tQDs, with their native hydrophobic ligands, cannot participate in the hydrogen bonding. This unfavorable ligand-polymer interaction leads to the observed tQD clusters in the polymer matrix (Figure 1C). Prior demonstrations of the tQD support the idea of partial stress transfer to the particle. Previously, tQDs were added to hydrophilic polymers, such as Nomex, through diffusion after application of a droplet of particle solution. Diffusion likely creates a weaker particle−polymer interface than electrospinning and explains why a smaller maximum particle shift was seen in previous work.[32] This suggests the tQD could also be used to optically probe the particle−polymer interface strength in composite materials. Future studies are planned to examine how controlled variation of interface strength affects agreement between fluorescence and UTM data.

Despite the incomplete stress transfer to the particle phase, the tetrapod fluorescence still clearly responds to fiber deformation. This demonstrates the tQD's usefulness in reporting phase-specific mechanical information in composite materials. Figure 3 illustrates schematically how the deformation is sensed by tQDs. The UTM load cell senses the macroscopic strain, while the tQD is only sensitive to nanoscale deformations that introduce a strain in the CdSe/CdS nanocrystal lattice. These latter deformations may arise from nanoscale particle−particle interactions (inter- and intra-aggregate interactions) or direct nanoscale particle−polymer interaction, but not from purely polymer molecular modes of deformation such as amorphous twist-tie chain unraveling, backbone covalent bond stretching, and others.[46] The phase-specific probing behavior of the tQD helps explain the differences between the optical and mechanical testing shown in Figure 2.

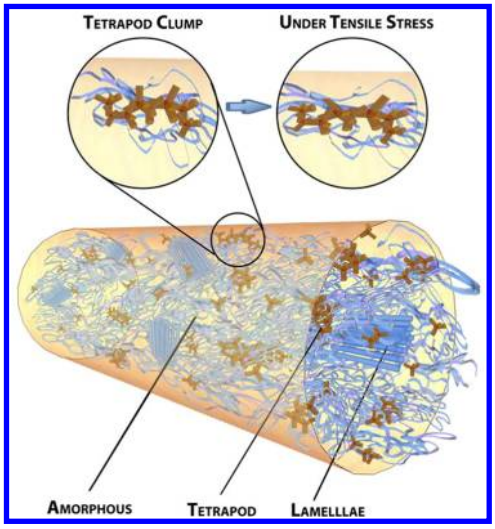

Figure 3. Schematic illustrating aggregation of tetrapods in PLLA fiber, as well as stress transfer to the aggregates during stretching.

Stress Relaxation. In service, parts often undergo more complex stress-states than pure tensile elongation, such as stress relaxation and hysteresis. These more complex behaviors are of key importance to understanding polymer dynamics. Therefore, with an eye toward applications and advanced fundamental studies, we also examined stress relaxation and hysteresis in the nanocomposite, both optically as well as mechanically. To the best of our knowledge, this has never been mapped using self-sensing nanoscale sensors embedded into a material. Figure 4A depicts the results of a mechanical tensile test in which a fiber containing 10% tetrapods by weight was stretched to 77% strain and held there for approximately 53 s. Stress is plotted as a function of time and shows an exponential falloff associated with stress relaxation in the polymer.[60] Figure 4B illustrates a fluorescence test performed under identical strain rate and holding conditions as the mechanical test. The same distinct exponential falloff in stress relaxation is seen. The stress relaxation tests in the UTM were performed on 5 fibers of each tQD concentration (15 fibers total) and no difference in load relaxation properties was observed as a function of concentration. The mechanical stress relaxation behavior showed a 28.8 ± 0.8% 30.2 ± 0.7%, and 29.9 ± 1.38% relaxation for fibers containing 3.6%, 10%, and 20% tetrapods by weight, respectively. The average over all 15 samples was 29.6 ± 1.13% relaxation. By contrast, the average over 45 fiber samples of stress relaxation measured optically was 20.9 ± 6.24% relaxation. Given that the mechanical test measures macroscale stress relaxation while the tetrapod sensing of stress relaxation originates from local nanoscale polymer deformations, the degree of agreement between the two measurements is striking and demonstrates that the tetrapod can be an effective nanoscale sensor for stress relaxation, in addition to tensile properties. This may be useful for a variety of applications as it demonstrates an optical means of determining stress relaxation prior to failure in structural materials. We observed a faster mechanical stress relaxation rate, (see Supporting Information, Figure S4, for exponential decay fits) consistent with the incomplete stress transfer to the tetrapod filler phase. In the case of the nanotetrapod−PLLA polymer nanocomposite, the load sensor is the filler phase and therefore only measures a fraction of the load felt by the polymer matrix. The smaller exponential stress falloff measured optically is thus in accord with the broadness of the linear response of the tQD as compared to that measured by the tensile testing machine, and further supports our proposed stress transfer explanation of differences between the two tests.

Cyclic Deformation. We also used the tQD as a probe for sensing the response of the single PLLA fibers to cyclic loading, again as compared to mechanical tests, and found telling differences between the hysteresis curves obtained via the two methods. Figure 5A shows a hysteresis loop done on a 10% tetrapod−PLLA composite fiber measured mechanically. The fiber was stretched to approximately 10% strain and returned to zero strain at the same strain rate; as before the same strain rates and test conditions were used with both sets of tests. The fiber shows clear hysteresis in the first cycle of the mechanical test (Figure 5A), but does not show hysteresis in the first optical test cycle (Figure 5B). If taken as a sensor of the polymer matrix, the tetrapod is reporting that some of the polymer plastic deformation is elastic. We believe that this again indicates that the tQD sensor is, in the PLLA nanocomposite

dx.doi.org/10.1021/nl401999t | Nano Lett. 2013, 13, 3915−3922

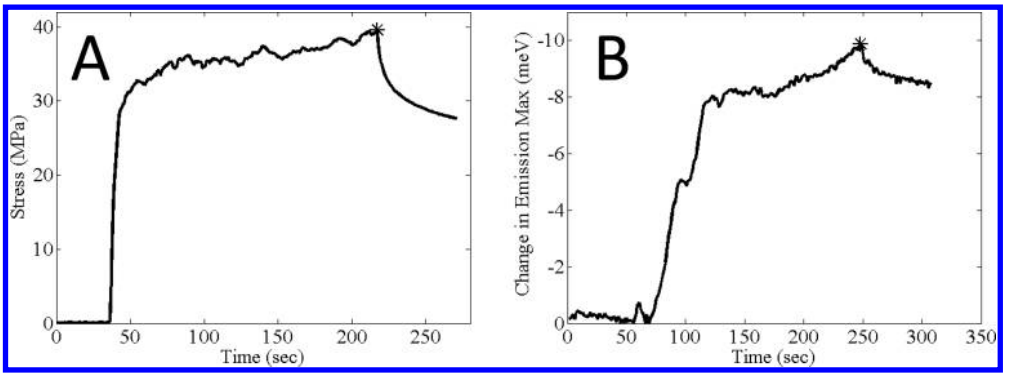

Figure 4. Comparison of load relaxation behavior between tetrapod probe and commercial tensile tester. (A) Macroscopic mechanical test data illustrating load relaxation. (B) Fluorescence test data obtained under same mechanical test conditions (strain rate, percent extension, and load relaxation time) illustrating load relaxation. ∗ indicates when strain was held at 77%.

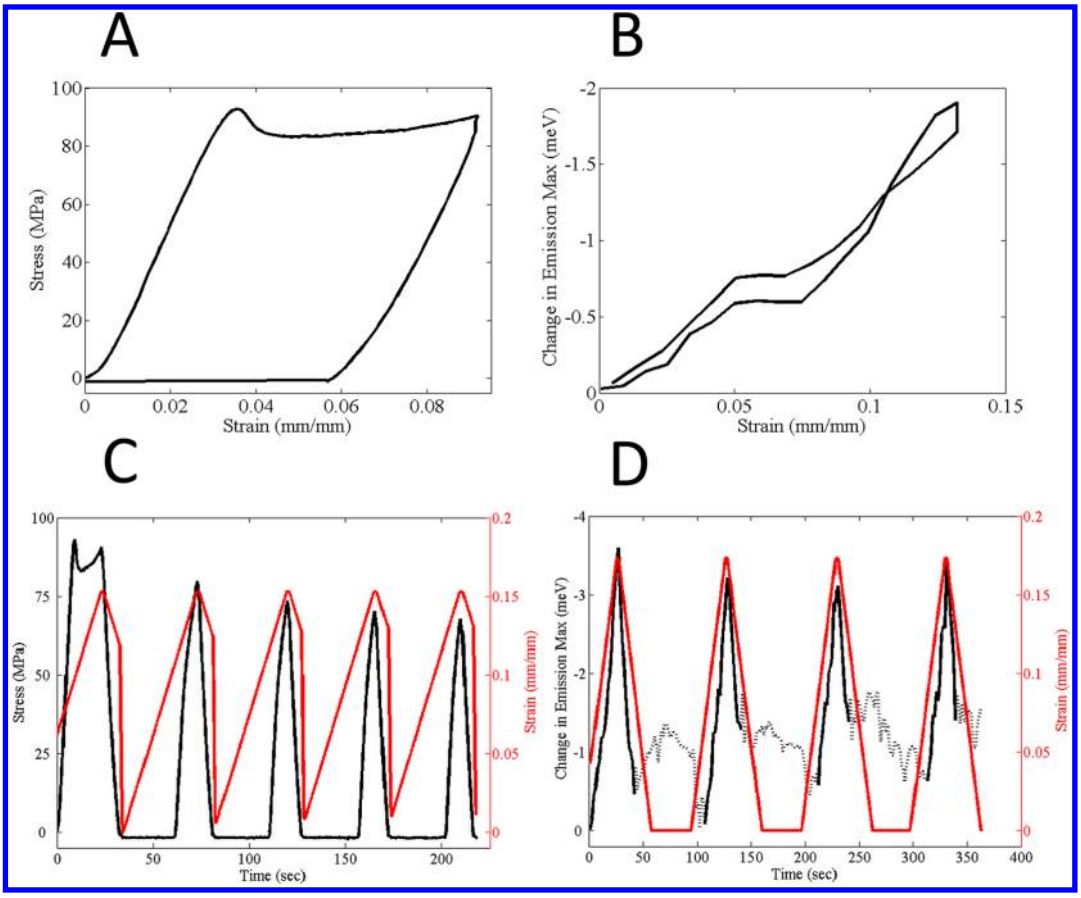

Figure 5. Comparison of hysteresis behavior between the macroscopic mechanical test and tQD probe. (A) Mechanical hysteresis loop illustrating plastic deformation and accompanying energy loss. (B) Fluorescence 'hysteresis' curve obtained under same mechanical test conditions (strain rate, percent extension, and return rate) illustrating little to no hysteresis. (C) Hysteresis loops from trials shown in part A plotted versus time. (D) Fluorescence 'hysteresis' loops of data from trials in plot B plotted versus time. Dashed regions indicate periods where fiber was not in focus due to slack from plastic deformation.

system, reporting the stress that is transferred to the particle phase rather than the stress felt by the matrix. Furthermore, the fluorescence shift is based on an elastic deformation of the tQD crystal lattice[34,35] and is not expected to show hysteresis.[33] The complete recovery of the initial width and position of the fluorescence signal also indicates the lack of residual stress in the tetrapod. Possibly, the poor particle−polymer interface, and the accompanying aggregation, may limit stress transfer to the tetrapods and prevent permanent deformation of the tetrapod probe.

Parts C and D of Figure 5 represent the trials shown in Parts A and B of Figure 5, respectively, only now as a function of time. In these plots, the clear resemblance between the latter cycles is shown, whereas the first cycle again displays plastic deformation. Figure 5D also illustrates a level of baseline optical noise present in between optical test cycles. The noise is due to the fiber coming out of focus between cycles. Upon plastic deformation, the fiber length increases, and so upon returning to zero strain between cycles, it goes out of focus.

dx.doi.org/10.1021/nl401999t | *Nano Lett.* 2013, 13, 3915−3922

As the cyclic deformation has nearly no hysteresis in the tetrapod fluorescence shift, no energy is dissipated in the tetrapods even when a great deal is lost in the polymer; this is evident through the degree of plastic deformation present in the mechanical hysteresis curves. These observations of hysteresis imply that in composites characterized by weak nanofiller-polymer interfaces, such as the nanocomposite material presented here, failure occurs due to cracking in the polymer matrix or particle−polymer interface rather than within the tetrapod nanoparticle phase. Through hysteresis data, the tQD therefore provides a simple imaging technique for determining the source of failure in a nanocomposite.

Conclusions. In summary, we have demonstrated that electrospun tQD−polymer composites provide a fluorescence-based measurement of tensile stress or strain in good agreement with results from traditional uniaxial tensile testing. With characteristics unique to tetrapod quantum dots, we have shown that they are capable of fluorescently monitoring the stress on a nanoscale component of a nanocomposite material. On the basis of this work, several key conclusions can be made:

- The elastic and plastic regions of deformation during extension are easily observed as a shift in the fluorescence of the tQD even at low particle concentrations, although a greater fluorescence shift per unit strain is observed with increasing concentration.
- Despite aggregation and poor stress transfer, the tQD shows close agreement with traditional tensile measurements. Far from problematic, this aggregation and accompanying weak interface may present an advantage; by limiting stress transfer to the tQD, it ensures accuracy and elasticity (recoverability and recyclability) by preventing plastic deformation of the tetrapod sensor.
- The tQD acts as a nonperturbing probe since electrospinning provides a straightforward means to form polymer-nanocrystal nanocomposites across a wide range of particle concentrations without adversely affecting the mechanical properties of the poly(L-lactic acid) matrix used in this study.
- We further show the capability of the tQD to monitor not only simple uniaxial stress, but stress relaxation and behavior under cyclic varying loads.

■ ASSOCIATED CONTENT

Supporting Information

Figures and tables including TEM images of different tQD-polymer composites and data on mechanical properties and dynamic scanning calorimetry. This material is available free of charge via the Internet at http://pubs.acs.org.

■ AUTHOR INFORMATION

Corresponding Author

*E-mail: (A.P.A.) alivis@berkeley.edu.

Author Contributions

[#]These authors contributed equally. The manuscript was written through contributions of all authors. All authors have given approval to the final version of the manuscript.

Notes

The authors declare no competing financial interest.

■ ACKNOWLEDGMENTS

Work on tetrapod nanocrystal−polymer nanocomposite electrospinning and optical, mechanical, and structural characterization was supported by the Director, Office of Science, Office of Basic Energy Sciences, Division of Materials Science and Engineering, of the U.S. Department of Energy under Contract DE-AC02-05CH11231, specifically on the Inorganic/Organic Nanocomposites NSET Program (to S.N.R., K.T., T.X., and A.P.A.). Support for mechanical characterization was provided by the Director, Office of Science, Office of Basic Energy Sciences, Division of Materials Science and Engineering, of the U.S. Department of Energy under Contract No. DE-AC02-05CH11231 (to B.G. and R.O.R). K.T. further acknowledges an NSF Graduate Fellowship. Electrospinning work was supported by the China Scholarship Council (2011619026) (to G.C)., and NSF Grant ECCS-0901864 (to L.L.). The authors would additionally like to thank Professor Ronald Gronsky for helpful discussions. They also thank Jim Litynski of Piezosystems Jena, Sheila Raja for help with the piezosystems D-Drive and piezodrive fiber stretcher, Jackson Huang, Amy Lu, and John Zhang for assistance with fiber diameter measurements, sample collection, and mechanical testing, Eric Granlund for machining of parts, and Phillip Agee and Sandip Basu of Agilent for their help with the Agilent T150 tensile tester; Prof. Lilac Amirav for providing some of the tetrapod samples; Jimmy Nelson for nanorod samples; Jesse Engel for helpful discussions and critical review of the manuscript, and Prof. Jill Millstone, Charina Choi, and Prof. Kristie Koski for helpful discussions.

■ ACKNOWLEDGMENTS

Work on tetrapod nanocrystal-polymer nanocomposite electrospinning and optical, mechanical, and structural characterization was supported by the Director, Office of Science, Office of Basic Energy Sciences, Division of Materials Science and Engineering, of the U.S. Department of Energy under contract DE-AC02-05CH11231, specifically on the Inorganic/Organic Nanocomposites NSET Program (to S.N.R., K.T., T.X., and A.P.A.). Support for mechanical characterization was provided by the Director, Office of Science, Office of Basic Energy Sciences, Division of Materials Science and Engineering, of the U.S. Department of Energy under Contract No. DE-AC02-05CH11231 (to B.G. and R.O.R). K.T. further acknowledges an NSF Graduate Fellowship. Electrospinning work was supported by the China Scholarship Council (2011619026) (to G.C), and NSF Grant ECCS-0901864 (to L.L.).

■ REFERENCES

(1) Bruns, N.; Pustelny, K.; Bergeron, L.; Whitehead, T.; Clark, D. *Angew. Chem.* **2009**, *121*, 5776−5779.
(2) Gibson, R. F. *Compos. Struct.* **2010**, *92*, 2793−2810.
(3) Noor, A. K.; Venneri, S. L.; Paul, D. B.; Hopkins, M. A. *Comput. Struct.* **2000**, *74*, 507−519.
(4) Lau, A. K.; Leng, J. *Multifunctional Polymer Nanocomposites*; CRC Press: Boca Raton, FL, 2010.
(5) Balazs, A. C.; Emrick, T.; Russell, T. P. *Science* **2006**, *314*, 1107−1110.
(6) Breuer, O.; Sundararaj, U. *Polym. Compos.* **2004**, *25*, 630−645.
(7) Byrne, M. T.; Gun'ko, Y. K. *Adv. Mater.* **2010**, *22*, 1672−1688.
(8) McCabe, J. F.; Walls, A. *Applied Dental Materials*; Blackwell: Oxford, U.K., 2009.
(9) Gibson, R. F. *Principles of Composite Material Mechanics*; CRC Press: Boca Raton, FL, 2011; Vol. *218*.
(10) Wardle, B. L.; Saito, D. S.; García, E. J.; Hart, A. J.; de Villoria, R. G.; Verploegen, E. A. *Adv. Mater.* **2008**, *20*, 2707−2714. Hasan, T.; Sun, Z.; Wang, F.; Bonaccorso, F.; Tan, P. H.; Rozhin, A. G.; Ferrari, A. C. *Adv. Mater.* **2009**, *21*, 3874−3899.

(11) Kim, J.; Kuk, E.; Yu, K.; Kim, J.; Park, S.; Lee, H.; Kim, S.; Park, Y.; Park, Y.; Hwang, C.; Kim, Y.; Lee, Y.; Jeong, D.; Cho, M. *Nanomed.: Nanotechnol., Biol. Med.* **2007**, *3*, 95−101.
(12) Smart, S.; Cassady, A.; Lu, G.; Martin, D. *Carbon* **2006**, *44*, 1034−1047.
(13) Ciprari, D.; Jacob, K.; Tannenbaum, R. *Macromolecules* **2006**, *39*, 6565−6573.
(14) Ciprari, D. L. *Mechanical Characterization of Polymer Nanocomposites and the Role of Interphase*. Ph.D. Dissertation, Georgia Institute of Technology, Atlanta, GA, 2004.
(15) Lewis, S. L. *Interface Control in Polymer Nanocomposites*. Ph.D. Dissertation, Rensslaer Polytechnic Institute, Troy, NY, 2007.
(16) Schadler, L. S.; Giannaris, S. C.; Ajayan, P. M. *Appl. Phys. Lett.* **1998**, *73*, 3842.
(17) Velasco-Santos, C.; Martinez-Hernandez, al; Castano, V. *Compos. Interfaces* **2005**, *11*, 567−586.
(18) De Wolf, I. *Semicond. Sci. Technol.* **1996**, *11*, 139−154.
(19) Sicardy, O.; Touet, I.; Rieutord, F.; Eymery, J. *J. Neutron Res.* **2001**, *9*, 263−272.
(20) Vaudin, M. D.; Gerbig, Y. B.; Stranick, S. J.; Cook, R. F. *Appl. Phys. Lett.* **2008**, *93*, 193116−193116−3.
(21) Rabe, U.; Janser, K.; Arnold, W. *Rev. Sci. Instrum.* **1996**, *67*, 3281−3293.
(22) Yamanaka, K.; Nakano, S. *Jpn. J. Appl. Phys.* **1996**, *35*, 3787−3792.
(23) Odegard, G.; Gates, T.; Herring, H. *Exp. Mech.* **2005**, *45*, 130−136.
(24) Liang, X.; Oldenburg, A. L.; Crecea, V.; Chaney, E. J.; Boppart, S. A. *Opt. Express* **2008**, *16*, 11052−11065.
(25) Kamat, N. P.; Liao, Z.; Moses, L. E.; Rawson, J.; Therien, M. J.; Dmochowski, I. J.; Hammer, D. A. *Proc. Natl. Acad. Sci.U.S.A.* **2011**, *108*, 13984−13989.
(26) Jin, X.; Götz, M.; Wille, S.; Mishra, Y. K.; Adelung, R.; Zollfrank, C. *Adv. Mater.* **2013**, *25*, 1342−1347.
(27) Stevenson, A.; Jones, A.; Raghavan, S. *Nano Lett.* **2011**, *11*, 3274−3278. Stone, J. W.; Sisco, P. N.; Goldsmith, E. C.; Baxter, S. C.; Murphy, C. J. *Nano Lett.* **2007**, *7*, 116−119.
(28) Kolle, M.; Lethbridge, A.; Kreysing, M.; Baumberg, J.; Aizenberg, J.; Vukusic, P. *Adv. Mater.* **2013**, *25*, 2239−2245.
(29) Fiore, A.; Mastria, R.; Lupo, M. G.; Lanzani, G.; Giannini, C.; Carlino, E.; Morello, G.; de Giorgi, M.; Li, Y.; Cingolani, R. *J. Am. Chem. Soc.* **2009**, *131*, 2274−2282.
(30) Talapin, D. V.; Nelson, J. H.; Shevchenko, E. V.; Aloni, S.; Sadtler; Alivisatos, A. P. *Nano Lett.* **2007**, *7*, 2951−2959.
(31) Manna, L.; Milliron, D. J.; Meisel, A.; Scher, E. C.; Alivisatos, A. P.; Meisel, E. C. *Nat. Mater.* **2003**, *2*, 382−385.
(32) Choi, C. L.; Koski, K. J.; Olson, A. C.; Alivisatos, A. P. *Proc. Natl. Acad. Sci. U.S.A.* **2010**, *107*, 21306−21310.
(33) Choi, C. L.; Koski, K. J.; Sivasankar, S.; Alivisatos, A. P. *Nano Lett.* **2009**, *9*, 3544−3549.
(34) Schrier, J.; Lee, B.; Wang, L. *J. Nanosci. Nanotechnol.* **2008**, *8*, 1994−1998.
(35) Fang, L.; Park, J. Y.; Cui, Y.; Alivisatos, P.; Shcrier, J.; Lee, B.; Wang, L.; Salmeron, M. *J. Chem. Phys.* **2007**, *127*, 184704−6.
(36) Medintz, I.; Uyeda, H.; Goldman, E.; Mattoussi, H.; Goldman, H. *Nat. Mater.* **2005**, *4*, 435−446.
(37) Reneker, D. H.; Yarin, A. L.; Fong, H.; Koombhongse, S. *J. Appl. Phys.* **2000**, *87*, 4531−4547.
(38) Yarin, A. L.; Koombhongse, S.; Reneker, D. *J. Appl. Phys.* **2001**, *90*, 4836−4846.
(39) Reneker, D. H.; Yarin, A. L. *Polymer* **2008**, *49*, 2387−2425.
(40) Behler, K.; Stravato, A.; Mochalin, V.; Korneva, G. *ACS Nano* **2009**, *3*, 363−369.
(41) Ko, F.; Gogotsi, Y.; Ali, A.; Naguib, N.; Ye, H.; Yang, G.; Li, C.; Willis, P. *Adv. Mater.* **2003**, *15*, 1161−1165.
(42) D'Almeida, J.; Monteiro, S.; Menezes, G.; Rodriguez, R. *J. Reinf. Plast. Compos.* **2007**, *26*, 321−330.
(43) Jin, S. H.; Park, Y.; Yoon, K. H. *Compos. Sci. Technol.* **2007**, *67*, 3434−3441.
(44) Li, D.; Wang, Y.; Xia, Y. *Adv. Mater.* **2004**, *16*, 361−366.
(45) Wu, X.; Salkovskiy, Y.; Dzenis, Y. A. *Appl. Phys. Lett.* **2011**, *98*, 223108.
(46) Callister, W. D. *Materials Science and Engineering: An Introduction*, 8th ed., Wiley: Hoboken, NJ, 2010.
(47) Lodha, P.; Netravali, A. N. *J. Mater. Sci.* **2002**, *37*, 3657−3665.
(48) Takagi, H.; Ichihara, Y. *JSME Int. J. Ser. A* **2004**, *47*, 551−555.
(49) Monette, L.; Anderson, M. P.; Ling, S.; Grest, G. S. *J. Mater. Sci.* **1992**, *27*, 4393−4405.
(50) Rezgui, F.; Swistek, M.; Hiver, J. M.; G'Sell, C.; Sadoun, T. *Polymer* **2005**, *46*, 7370−7385.
(51) Elliott, D. M.; Narmoneva, D. A.; Setton, L. A. *J. Biomech. Eng.* **2002**, *124*, 223−228.
(52) Patidar, D.; Agrawal, S.; Saxena, N. *J. Polym. Eng.* **2010**, *30*, 565−574.
(53) Agarwal, S.; Patidar, D.; Saxena, N. *Polym. Eng.* **2012**, No. in press.
(54) Mathur, V.; Dixit, M.; Rathore, K.; Saxena, N.; Sharma, K. *Front. Chem. Sci. Eng.* **2011**, *5*, 258−263.
(55) Kaur, H.; Banipal, T.; Thakur, S.; Bakshi, M.; Kaur, G.; Singh, N. *ACS Sustainable Chem. Eng.* **2013**, *1*, 127−136.
(56) Liu, H.; Webster, T. J. *Int. J. Nanomed.* **2010**, *5*, 299−313.
(57) Marom, G.; Fischer, S.; Tuler, F. R.; Wagner, H. D. *J. Mater. Sci.* **1978**, *13*, 1419−1426.
(58) Voigt, W. *Lehrbuch der Kristallphysik*; B.G. Teubner: Leipzig, Germany, 1910.
(59) Reuss, A. *Z. Angew. Math. Mech.* **1929**, *9*, 49−58.
(60) Tobolsky, A. V. *J. Appl. Phys.* **1956**, *27*, 673−685.